International Journal of Radiation Oncology biology • physics

www.redjournal.org

Physics Contribution

Plan Selection in Proton Therapy of Locally Advanced Prostate Cancer with Simultaneous Treatment of Multiple Targets

Sara Pilskog, PhD,*,† Bonny Abal, MSc,† Kaja S. Øvrelid,* Grete May Engeseth, MSc,* Kristian S. Ytre-Hauge, PhD,† and Liv B. Hysing, PhD*,†

*Department of Oncology and Medical Physics, Haukeland University Hospital, Bergen, Norway; and †Institute of Physics and Technology, University of Bergen, Bergen, Norway

Received Mar 19, 2019. Accepted for publication Nov 7, 2019.

Summary

This study presented a method of plan selection in intensity modulated proton therapy to address the challenge of delivering treatment to the prostate and the pelvic lymph nodes with different motion patterns. The plan library used different positions of the prostate created from a population model of day-to-day target motion. Plan selection from this library reduced the dose to the rectum and bladder without compromising target coverage compared with nonadaptive delivery.

Purpose: Intensity modulated proton therapy (IMPT) of locally advanced prostate cancer can spare the bowel considerably compared with modern photon therapy, but simultaneous treatment of the prostate (p), seminal vesicles (sv), and lymph nodes is challenging owing to day-to-day organ motion and range uncertainties. Our purpose was, therefore, to generate a plan library for use in adaptive IMPT to mitigate these uncertainties.

Methods and Materials: We retrospectively included 27 patients with a series of computed tomography scans throughout their treatment representing day-to-day variation. In 18 of the patients, target motion was analyzed using rigid shifts of prostate gold markers relative to bony anatomy. A plan library with different p and sv planning target volume (p/sv-PTV) positions was defined from the distribution and direction of these shifts. Delivery of IMPT using plan selection from the library was simulated for image guidance on bony anatomy, in the remaining patients and compared with nonadaptive IMPT.

Results: The plan library consisted of 3 small margin p/sv-PTVs: (1) p/sv-PTV shifted 1.5 systematic error (Σ) of the population mean in the anterior and cranial directions, (2) p/sv-PTV shifted 1.5Σ in the posterior and caudal directions, and (3) p/sv-PTV in the planning position. The conventional p/sv-PTV was also available for backup. Plan selection compared with nonadaptive IMPT resulted in a reduction of the rectum volume receiving 60 Gy relative biological effect (RBE) ($V60_{GyRBE}$) from on average 12 mL to 9 mL. For the bladder the average $V45_{GyRBE}$ was reduced from 36% to 30%. Large and small bowel doses were also reduced, whereas target coverage was comparable or improved compared with nonadaptive IMPT.

Corresponding author: Sara Pilskog, PhD; E-mail: sara.thornqvist@uib.no

The Trond Mohn foundation (grant numbers BFS2017TMT07 and BFS2015TMT03) is acknowledged by the project for funding the research of Thörnqvist, Engeseth and Ytre-Hauge. The first author of this work has also been supported by research grants from the Norwegian Cancer Society.

Disclosures: none.

Supplementary material for this article can be found at https://doi.org/10.1016/j.ijrobp.2019.11.007.

Acknowledgments—Senior oncologist Svein Inge Helle is acknowledged for manual contouring of the CT data.

Int J Radiation Oncol Biol Phys, Vol. 106, No. 3, pp. 630–638, 2020

https://doi.org/10.1016/j.ijrobp.2019.11.007

Conclusions: Plan selection based on a population model of rigid target motion was feasible for all patients. Compared with conventional IMPT, plan selection resulted in significant dosimetric sparing of rectum and bladder without compromising target coverage.

Introduction

Day-to-day organ motion is a challenge for accurate treatment delivery in modern radio- and especially in intensity modulated proton therapy (IMPT). The greater sensitivity to motion for protons is due to their finite range in addition to elevated dose deposited at the end of their paths, which can cause deterioration of the dose distribution if the planning anatomy deviates from the treated. For passive scattering proton therapy (PT) of localized prostate cancer, both variations in bony anatomy (BA) and soft-tissue deformation prevent margin reductions.[1] In prostate cancer, the benefits of PT from increased dose conformity lead to normal tissue sparing, and in regard to bowel could be greater for locally advanced than for localized disease.[2] Still, margins to account for target motion may cause high exposure of surrounding organs at risk while resulting in unsatisfactory dose coverage of the target.[3,4] The addition of the pelvic lymph nodes further increases the treatment complexity because the motion of the pelvic lymph nodes differs from those of the prostate and seminal vesicles.[3,5-8]

One method to limit the impact of day-to-day organ motion is through an adaptive delivery approach. In adaptive PT of prostate cancer, simulation studies have mainly concerned online replanning.[4,9,10] Online replanning has also been studied for photon radiation therapy, but the additional workload required, for example, for contouring and plan quality assurance, has obstructed the vast majority of the simulation studies from reaching clinical practice.[11] Plan selection has, however, been implemented successfully across several pelvic sites and enabled normal tissue sparing in photon radiation therapy.[12-17] For locally advanced prostate cancer, Xia et al constructed a plan library for rigid shifts of the prostate relative to the pelvic lymph nodes for 1 patient to reduce rectum dose.[12] This plan selection procedure has the potential to reduce the impact of range uncertainty in PT caused by altered bony anatomy[1] while reducing target margins. In our study, we wanted to describe a method of deriving a plan library using conventional margin recipe for motion and evaluate the potential in IMPT. We hypothesize that selection from a plan library with different positions of the prostate and seminal vesicle planning target volumes (p/sv-PTV) in relation to the lymph node target can improve sparing of normal tissue while maintaining coverage for all targets compared with nonadaptive IMPT.

Methods and Materials

The study included 27 patients previously treated for locally advanced prostate cancer with intensity modulated radiation therapy (IMRT). The regional ethical committee of western Norway approved the original dose escalation study and each patient gave an informed consent before participation to undergo additional imaging. Each patient was represented by a planning computed tomography (pCT) and 6 to 10 repeat CTs (rCTs) (average: 9 rCTs) acquired evenly throughout the course of treatment, roughly corresponding to 2 rCTs per full treatment week and avoiding scans on successive days. All patients had 3 fiducial gold-markers (GMs) implanted in the prostate before acquiring the pCT, and the course of IMRT was delivered with image guidance primarily on GM with translational correction of the patient position. For the pCT, bladder contrast was injected to aid bladder and prostate differentiation (contrast overwritten to water equivalent for planning). Identical patient fixation was for all CTs and no laxatives administrated.

Three targets were defined in the pCTs and in the rCTs: the prostate clinical target volume (p-CTV) as the prostate gland including capsule and possible extraglandular tumor extension, the combined prostate and seminal vesicle CTV (p/sv-CTV) as the p-CTV extended with seminal vesicles, and the lymph node CTV (ln-CTV) as the p/sv-CTV extended with pelvic lymph nodes. The lymph nodes were contoured according to Radiation Therapy Oncology Group guidelines, but omitting the presacral nodes.[6] Additionally, organs at risk were contoured in all CTs with bladder and rectum manually segmented to encompass organ with content.[18] Large bowel was defined from the cranial end of the rectum to above the cranial part of the lymp node PTV (ln-PTV) and included sigmoid and descending colon. Small bowel was defined as the remaining bowel loops within the cranio-caudal extensions of the large bowel. Further details on the patient material and the IMRT treatment procedure for these patients can be found elsewhere.[19,20]

The population-model of day-to-day motion for plan library construction

The patients were partitioned into a training set consisting of the first 18 patients and a testing set consisting of the 9 remaining patients. From the training set, a day-to-day

motion model was derived describing the movement of the p-CTV in relation to ln-CTV, substituted by the intraprostatic GMs and pelvic BA, respectively. The global translation in the lateral, longitudinal, and vertical directions to align each rCT i ($i = 1…N$) to the pCT for every patient, k ($k = 1…18$) was described by the vector, $\boldsymbol{v}_{GM}^{i,k}$ for GM- and $\boldsymbol{v}_{BA}^{i,k}$ for BA-based registrations. The residual motion vector, $\boldsymbol{v}_{res}^{i,k} = \boldsymbol{v}_{GM}^{i,k} - \boldsymbol{v}_{BA}^{i,k}$ was assumed to capture the residual motion of the p-and p/sv-CTVs relative to the ln-CTV when positioning the patient on BA. In total, 160 rCTs were used to quantify the residual motion vector. The normality of the motion was checked visually by Quantile-Quantile plots and histograms.

The magnitude of p- and p/sv-CTV day-to-day motion in the patient population was estimated from the systematic uncertainty ($\boldsymbol{\Sigma}$) and random ($\boldsymbol{\sigma}$) uncertainties, commonly used in margin recipes.[21,22] The $\boldsymbol{\sigma}$ was, therefore, estimated as the root-mean-square of the patient-specific standard deviation of $\boldsymbol{v}_{res}^{k} = \frac{1}{N}\sum_{i}\boldsymbol{v}_{res}^{i,k}$. The systematic difference in residual motion between planning and treatment, $\boldsymbol{\Sigma}$ was calculated as the direction-specific standard deviation of the population-average residual motion, $\boldsymbol{v}_{res} = \frac{1}{18}\sum_{k}\boldsymbol{v}_{res}^{k}$. For the conventional plan used in the nonadaptive delivery, the p- and p/sv-CTV were expanded according to van Herk et al securing high (>95%) target coverage in 90% of the population.[22] This plan also was used for backup in the plan library and will hereafter also be referred to as "the backup plan." Our purpose was to differentiate the day-to-day motion using displaced positions of the p-and p/sv-CTV such that, instead of having a large PTV accounting for most of the residual motion, patients with greater systematic error (or instances with large residual motion) would be treated with a displaced CTV. The factor of the systematic error determines the fraction of patients who receive dose above a certain threshold.[22] The PTV expansion was, therefore, reduced to cover 50% of the population instead of 90% by changing the factor of the systematic error from 2.5 to 1.5 and neglecting random uncertainties. The selected 50% confidence level was a compromise between our intention to have the original position selected most frequently but yet avoid a large PTV and instead have the displaced targets selected for the outlier positions or large residual motion. The PTV expansion due to motion was for simplicity used for all plans (except for the backup plan) in the library.

Similarly, the displaced p-and p/sv-CTVs were obtained by translating the original p-and p/sv-CTV position by $\pm 1.5\boldsymbol{\Sigma}$. To facilitate the manual plan selection, we wanted to reduce the number of plans in the library as much as possible without compromising prediction of the most probable p/sv-CTV positions. This was done by analyzing the pairwise correlation of $\boldsymbol{v}_{res}^{i,k}(x,y), \boldsymbol{v}_{res}^{i,k}(x,z), \boldsymbol{v}_{res}^{i,k}(y,z)$ and adapting the displaced positions to account for possible correlations. Furthermore, displacements less than 3 mm in any of the anatomic directions were neglected as a pragmatic solution to reduce the number of treatment plans in the library.

The resulting plan library consequently contained plans with a linear combination of p- and p/sv-PTV positions along the main directions of day-to-day motion in addition to 2 p- and p/sv-PTVs—1 with a small and 1 with a conventional margin—in the original planning position. IMPT with the nonadaptive delivery of the conventional plan was subsequently compared with the adaptive approach of plan selection from the constructed libraries.

Treatment planning and delivery simulations

The nonadaptive and adaptive approach of treatment delivery was simulated for 9 testing patients. For these patients, IMPT plans with 2 lateral opposing fields and a constant relative biological effect (RBE) of 1.1 were optimized in Eclipse treatment planning system (Varian medical systems, Palo Alto, US). The prescription for all plans was 67.5 Gy(RBE) to the p-PTV, 60 Gy(RBE) to the p/sv-PTV, and 50 Gy(RBE) to the ln-PTV delivered as a simultaneous integrated boost in 25 fractions. As previously described, the p-and p/sv-PTVs were defined using the population-model for both the adaptive and nonadaptive delivery approaches. In the plan library, only the p- and p/sv-PTVs were shifted on the pCT, with the segmentation for the rectum, bowel, and intestine remaining unchanged. The ln-PTV was expanded isotopically by 5 mm for both delivery approaches, based on results from previous motion studies.[5,23] Field-specific lateral, proximal, and distal margins used for IMPT planning to increase robustness were 10 mm, 1 mm, and 2 mm, respectively.

All plans (original p- and p/sv-PTVs and those shifted) had the goal to satisfy the following dose criteria (in order of prioritisation): PTV $D_{98\%} > 95\%$ of the prescribed dose, rectum $V_{60GyRBE} < 10$ mL, bladder $V_{45GyRBE} < 35\%$, intestine, that is, the defined small and large bowel loops $V_{40GyRBE} < 30\%$.

For treatment simulation, the IMPT plans of the pCT were transferred to the rCTs using BA registration followed by dose recalculations such that the planned proton fluences and spot distribution were delivered for the new patient geometry. For the nonadaptive approach, only the plan with conventional margins was available for treatment. The adaptive approach used a selection of plans from the libraries. The plans with p/sv-PTV that geometrically encompassed the p/sv-CTV in each of the rCT were selected for treatment. If this was fulfilled by several PTVs in the library, the one with least geometric amount of overlap with the organs at risk of the rCT was selected. All selections were made visually, and to evaluate consistency of the procedure, the selection was made independently by 2 medical physicists and differences were reviewed for agreement. Only the selected plan was transferred to the rCT followed by a dose recalculation. The dose recalculations were performed subsequent to all selections and blinded to the physicists making the selections.

The simulated dose delivered with the adaptive and the nonadaptive approach was compared for all CTVs using $D_{98\%}$ and for organs at risk using generalized equivalent uniform dose (gEUD) for rectum (with the volume factor, k = 12), bladder (k = 8), small (k = 4), and large bowel (k = 4) in addition to the dose criteria used for planning. The obtained dose-volume parameters ($D_{98\%}$, $V_{60GyRBE}$, $V_{45GyRBE}$, $V_{40GyRBE}$,) and gEUD from each rCTs were averaged for all rCTs and patients, and these distributions were checked for normality before statistical testing. The averages of the dose parameters from the adaptive and the nonadaptive approach were compared with a paired test (*t* test for normally distributed data and Wilcoxon signed rank for non-normal data) with significance of $P \leq .05$.

Results

Plan library composition

The greatest variation of residual p- and p/sv-CTV motion was seen in the anterior−posterior and the caudal−cranial direction, both with **Σ** of 3 mm, whereas the **Σ** for right−left motion was less than 1 mm (Fig. E1; available online at https://doi.org/10.1016/j.ijrobp.2019.11.007). Noticeable linear correlation was only found in the caudal−cranial and anterior−posterior directions; the regression coefficient was 0.7 mm^{-1} with a moderate coefficient of determination, $R^2 = 0.53$ (Fig. 1A, Fig. E2; available online at https://doi.org/10.1016/j.ijrobp.2019.11.007). Applying the preset displacement factor of ±1.5**Σ** to the original p- and p/sv-CTV positions in the anterior−posterior direction resulted in shifts of ±5 mm. In the caudal−cranial direction, this shift combined by the regression resulted in shifts of ±3 mm. Because 1.5**Σ** in the right−left direction resulted in a displacement of only 1 mm, it was neglected. The plan library, therefore, consisted of 2 shifted p- and p/sv-CTV positions: (1) 5 mm posteriorly and 3 mm caudally referred to as "plan down" and (2) 5 mm anteriorly and 3 mm cranially referred to as "plan up" (Fig. 1B, Fig. 2). In addition to the shifted targets, the original position of the p- and p/sv-CTVs, denoted "plan mid," was included in the plan library. The PTV margin for these targets, using 1.5**Σ** was 5 mm in the direction of the largest residual motion. This expansion was applied to all directions owing to other uncertainties, for example, from delineation and intrafraction motion.

The motion described by the population model applied to the margin recipe resulted in PTV margins of 3 mm in the right−left direction and 10 mm elsewhere for p- and p/sv-CTVs of the conventional or backup plan. The 3 mm margin in the right−left direction purely derived from motion were, using the same arguments on additional uncertainties as for the margins applied to the plans in the plan library, deemed too small and was replaced by a 5 mm expansion.

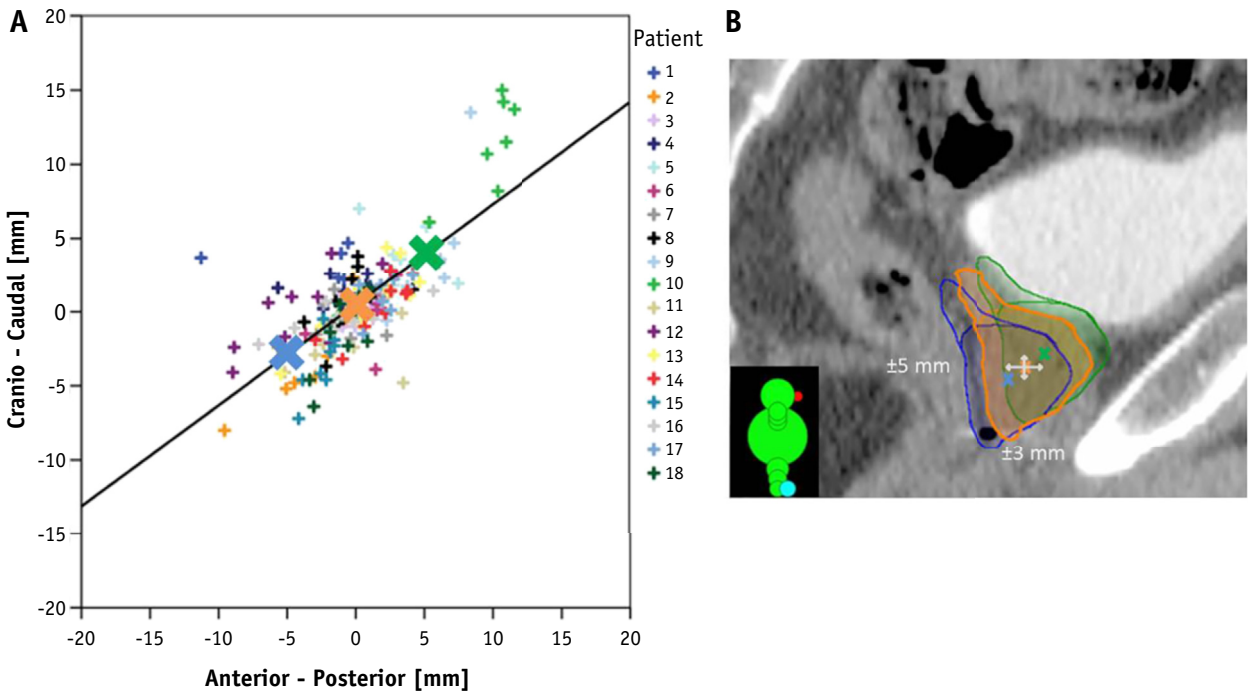

Fig 1. Creation of the plan library. (A) The difference in gold-marker− and bony anatomy−based shifts for all training patients denoted with crosses of different colors. Large crosses describe the position of the high-dose clinical target volume (CTV) with plan up (green), plan mid (orange), and plan down (blue). (B) Target positions as crosses together with prostate, seminal vesicles CTV in a testing patient. Gray arrows with numbers describe translations of the displaced CTVs. (A color version of this figure is available at https://doi.org/10.1016/j.ijrobp.2019.11.007).

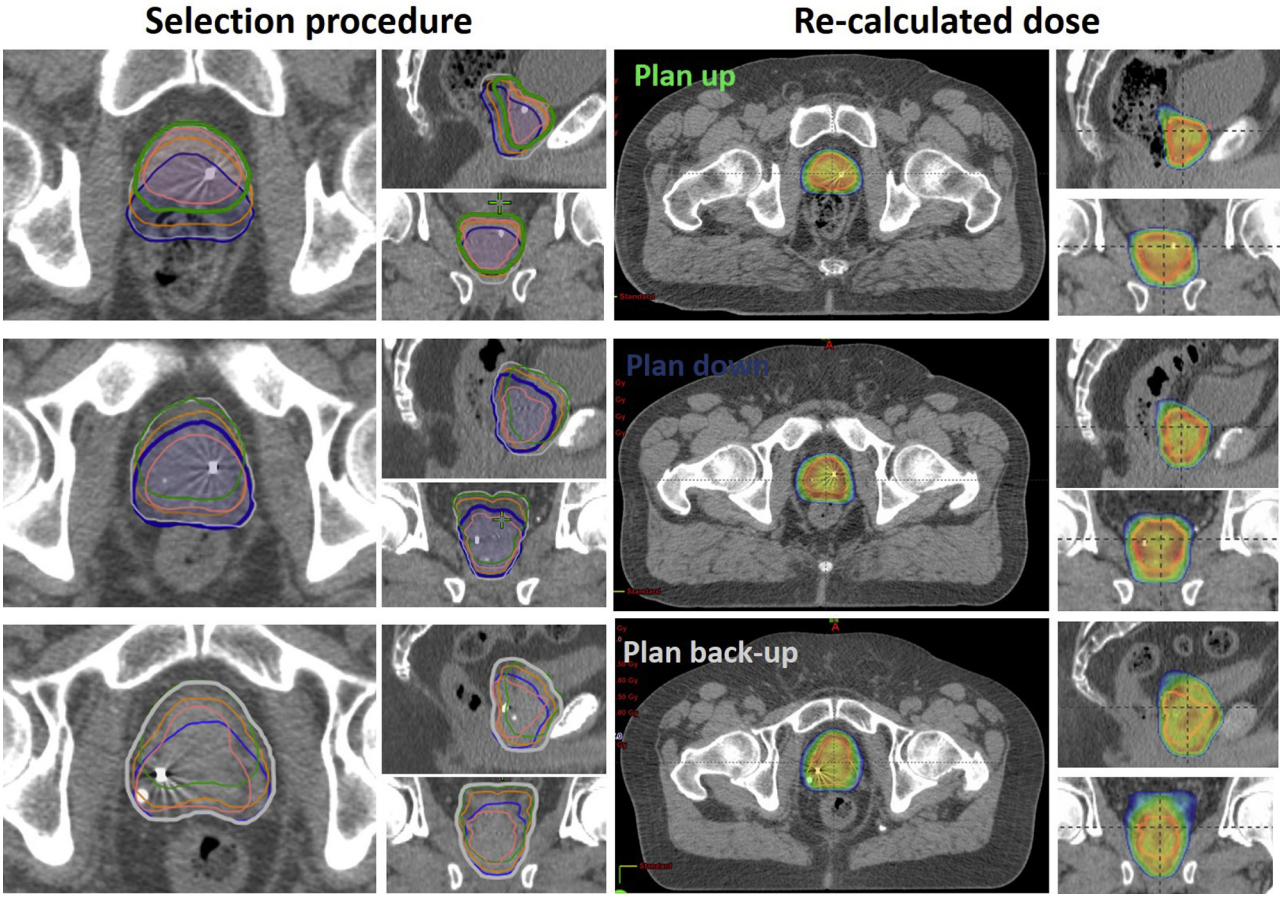

Fig. 2. Examples of plan selection after the bony anatomy match of the repeat computed tomography to the plan computed tomography in patient 20 (top), 23 (middle), and 25 (bottom). Selected plans are visualized with bold contours (left column), with color coding the same as for Figure 1 and backup plan in gray. The dose distribution of the selected plans is shown with a 95%-dose threshold (right column). (A color version of this figure is available at https://doi.org/10.1016/j.ijrobp.2019.11.007).

When constructing the plan library for the testing patients, the large conventional margins of the nonadaptive delivery led to the plan evaluation criteria for both rectum and bladder being exceeded in 4 patients in addition to being exceeded for either rectum or bladder in another 2 patients. The dosimetric results from the IMPT planning further revealed that for plan down, the rectum criterion was violated in 5 patients, whereas for plan up the bladder criterion was exceeded in 5 patients. For plan mid, 1 patient did not meet the bladder criterion.

Plan selection frequencies and dosimetric comparison to the nonadaptive delivery

The most frequently selected plan across all patients was plan mid (45%) followed by the backup plan (30%), whereas plan down or plan up were less frequently used (16% and 9%, respectively). Two patients never had the backup plan selected, and no patients had both plan up and plan down chosen during the PT course (Fig. 3). As for the training patients, the difference in shifts from the GM- and BA-based registrations for the testing patients were correlated in the anterior−posterior and cranio-caudal directions (Fig. E3; available online at https://doi.org/10.1016/j.ijrobp.2019.11.007). When comparing the selected plans to the shifts in these directions the following patterns were seen. Plan mid was selected for motion in any of these directions <2 mm (true for 83% of these selections), plan down or plan up were selected for the anterior−posterior motion >2 mm (posteriorly for plan down and anteriorly for plan up) and larger than the motion in the cranio-caudal direction (true for 85% of these selections).

The treatment simulations showed significant ($P < .001$) sparing of rectum gEUD from an average of 56 ± 4 Gy(RBE) to 54 ± 5 Gy(RBE) with plan selection (Fig. 4, 5). Also, rectum $V_{60GyRBE}$ was significantly decreased from a median of 12 mL for the nonadaptive delivery to 9 mL ($P < .001$) with adaptive approach leading to 20% fewer rCTs where the plan criterion $V_{60GyRBE} < 10$ mL was violated. A significant dosimetric gain was also evident for the bladder with the average gEUD and $V_{45GyRBE}$ being 54 ± 4 Gy(RBE) and 36% for the nonadaptive and 52 ± 5

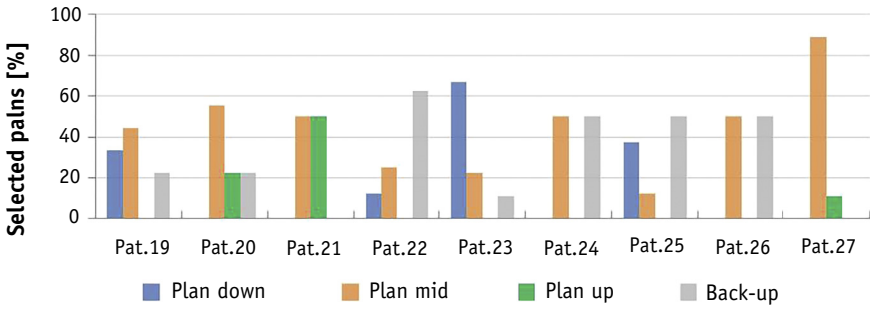

Fig. 3. Histogram of plan selection frequency in each of the testing patients.

Gy(RBE) and 30% for adaptive delivery ($P < .001$) (Fig. 5). The number of rCTs where the bladder planning criterion was violated was reduced by almost 40% with plan selection compared with the nonadaptive delivery. For both the small and large bowel, $V_{45GyRBE}$ were well below the planning criteria. The gEUD for the large and small bowel were however reduced by 4 Gy(RBE) using plan selection, whereas no differences were seen for the high-dose regions ($V_{60GyRBE}$) (Fig. E4; available online at https://doi.org/10.1016/j.ijrobp.2019.11.007).

The p/sv-CTV had the greatest improvement from the adaptations with coverage ($D_{98\%}$) on average 1 Gy(RBE) higher with plan selection compared with the nonadaptive delivery ($P < .001$) (Fig. 3, 4). A slightly higher coverage was also obtained for p/sv-CTV (Fig. 5). The $D_{98\%}$ for ln-CTV was similar between the 2 delivery approaches, but whereas the planning criterion of $D_{98\%} > 47.5$ Gy(RBE) was fulfilled in all rCTs with plan selection, it was violated in 20% of the rCTs with the nonadaptive delivery (Fig. E4; available online at https://doi.org/10.1016/j.ijrobp.2019.11.007).

Discussion

We have presented the potential of plan selection in IMPT of multiple targets. With our method of plan library construction, the original prostate position of the pCT would be most frequently used and plan up and plan down dedicated to outlier positions. This was also reflected in our results with plan mid being most frequently selected and with only 2 patients having the outlier plans selected for 50% or more of the simulated fractions (Fig. 3). Plan mid was most commonly the second-best match for the rCTs when the backup plan was selected. Choosing a larger confidence level by increasing the factor of the systematic error in combination with increasing the PTV margins for the original CTV position would be closer to the conventional approach of delivery with the outlier plans selected less frequently. In our study, the PTV expansion approximately corresponded with the amount of shift applied to the outlier positions, but no less than 5 mm and symmetrical owing to other uncertainties, as discussed below. Also, the PTV expansion was identical for all plans in the library, which is a simplification because the systematic and random components may be different for the outlier positions compared with the original position. Main reasons for selecting the backup plan were geometric misses from plan mid posteriorly or cranially. No obvious common cause for the geometric misses was present, but target deformation mainly owing to altered rectum shape, rotated pelvic, and delineation uncertainties were contributions.

The plan libraries were based on a simple motion model restricted to rigid translation of the p- and p/sv-targets in relation to the BA. The seminal vesicles, however, undergo deformations,[23] yet delivery with plan selection resulted in a high dose to this target (Fig. 5). Owing to deformations and other uncertainties from intrafraction motion and delineation, the smallest margins were set to 5 mm. Intrafraction motion for the prostate has been thoroughly studied and reported to rarely be >5 mm.[24,25] Delineation uncertainties for the ln-CTV can be considerable,[26] and to limit these uncertainties, all target delineations were made by 1 oncologist. Yet, a 5 mm margin may be considered at the lower end of what is acceptable for the ln-CTV. The motivation behind varying the position of the high-dose target was the assumption that range uncertainties will be limited by keeping the beam positions relative to BA constant throughout the course of treatment. Alternatively, the method used in this study could be applied for GM registrations instead, with the residual motion of the ln-CTV either handled by a larger PTV or by a plan library.

Dose degradation owing to BA variations for passive scattering PT using lateral fields and image guidance on prostate was reported by Trofimov et al, who found a correlation of femur angle and distal proton range for their target (prostate and seminal vesicles).[1] BA alterations were also found to contribute to reduced dose coverage of the prostate and seminal vesicle target in passive scattering PT using anterior-oblique fields with image guidance on prostate.[27] When comparing image guidance on BA versus guidance on the prostate-rectal wall, Maeda et al found superior or comparable target coverage for the latter.[28] In their study, the passive scattering technique was, however, planned to compensate for prostate motion of ±10 mm in relation to the BA, which was more than the recorded differences between the 2 setup techniques in their patient material. In our training material, such large motion was rare (2.5%) and nonexistent among the testing patients

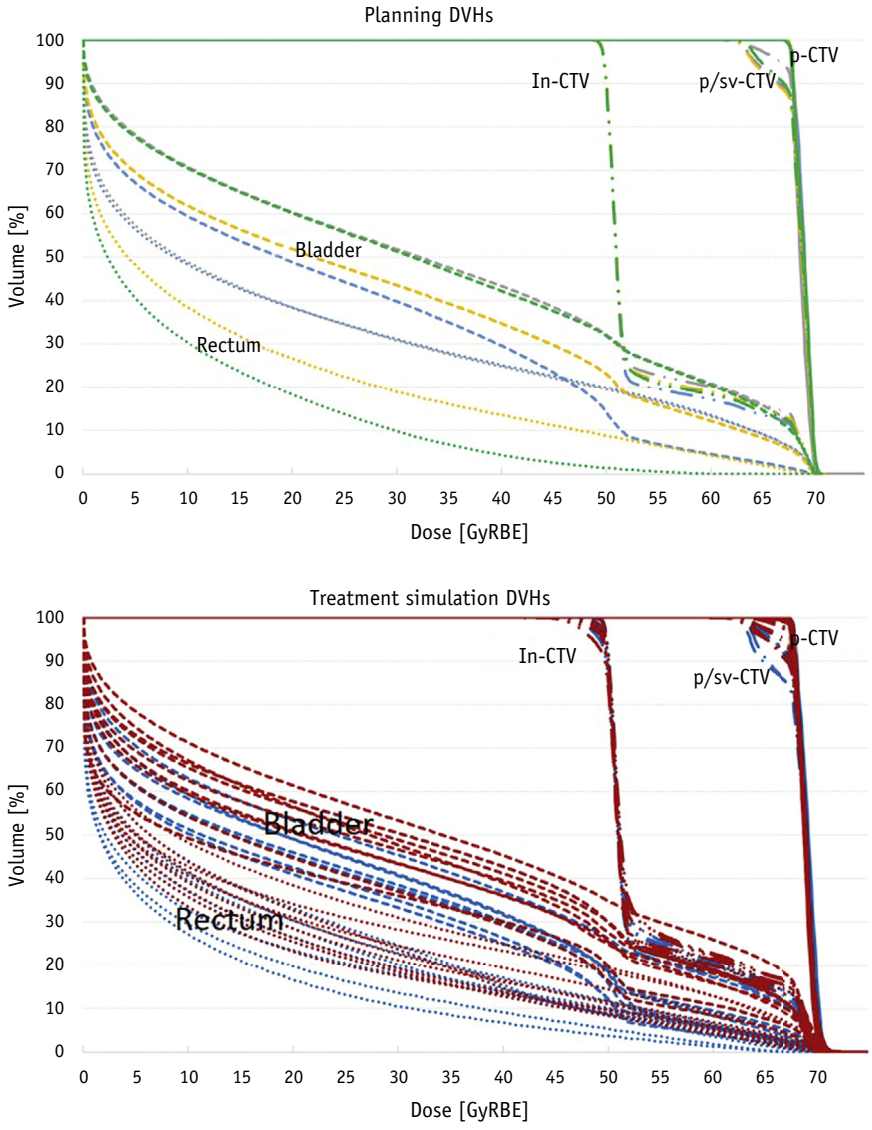

Fig. 4. Dose-volume histograms for patient number 19. The top image displays the planning dose-volume histograms for plan up (green), plan mid (orange), plan down (blue) and the nonadaptive plan also used for backup (gray). The bottom image shows treatment simulations for plan selection (blue) and nonadaptive delivery (red). The different line patterns for targets and organs at risk for both the top and bottom image are as described for the top image. (A color version of this figure is available at https://doi.org/10.1016/j.ijrobp.2019.11.007).

(Fig. 1, Fig. E1-E2; available online at https://doi.org/10.1016/j.ijrobp.2019.11.007).

Positioning on BA should be more beneficial for the pelvic lymph nodes because of their close location to the sacrum and pelvic girdle.[5] The ln-CTV was, however, the target with largest dose degradation in the rCTs with 2 patients having patient-average $D_{98\%}$ CTV <95% of the prescribed dose independent of delivery approach. The low-dose regions of the ln-CTV were commonly in the caudal parts of the target, at the boundary of the rectum and bladder. Our assumption to limit range uncertainties solely through BA positioning was, therefore, not sufficient for the ln-CTV. Reasons are likely multifactorial, influenced by rotations of the pelvic or femur and changes in body contour or bladder/rectum filling. For IMPT planning in the current version of our commercial planning system, target specific margins in the proximal, distal, and lateral direction was defined as a fixed distance instead of relative. In comparison to other generic margins (for passive scattering delivery), for example, 2.7% to 4.6% + 1.2 mm as in Paganetti[29] the PT specific range margins were around 2% for ln-PTV but closer to 1% in p- and p/sv-PTV, whereas our setup/motion margins were greater. Our margins were, however, comparable to previous studies on prostate when combining the proximal and distal margins with the PTV margins.[30,31]

Target specific range uncertainty margins and other beam configurations could potentially have reduced the amount of dose deformation. For the pelvic lymph nodes,

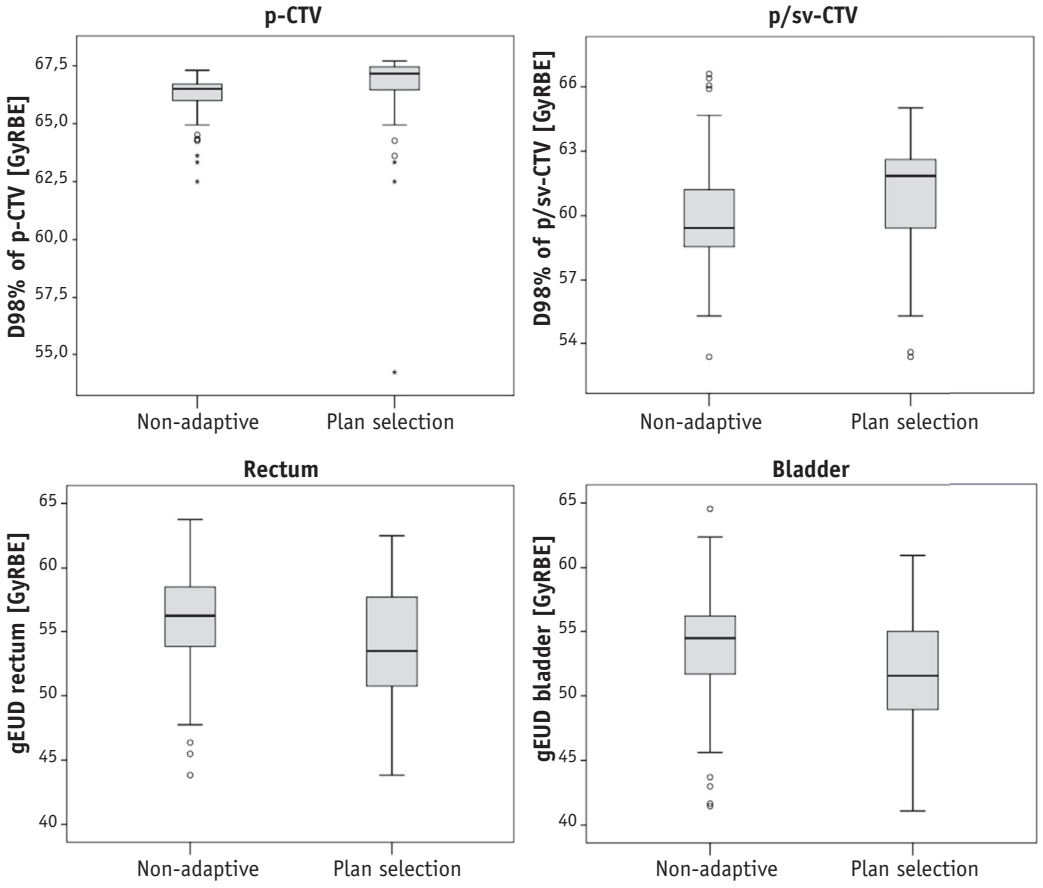

Fig. 5. Dosimetric evaluation of the high-dose clinical target volume (top) and rectum and bladder (bottom). Subplots show dose parameters for all repeat computed tomography in all patients from nonadaptive delivery (left) and plan selection (right). Shaded regions represent interquartile range, black line the median, whiskers the 95% confidence interval, and circle/stars outliers. For targets the dose to 98% of the clinical target volume ($D_{98\%}$), whereas for the organs at risk the generalized equivalent uniform dose using a volume factor (k) of $k = 12$ for the rectum and $k = 8$ for the bladder are shown.

range uncertainties quantified by the water equivalent path length of protons have been investigated for a wide range of beam angles.[32] This study was conducted on patient material (ie, pCT and rCTs) collected in the same trial as the material of the current study. Interestingly, lateral fields were, for the majority of the patients, associated with the greatest proton range variations, and anterior oblique or posterior oblique fields were found most robust.[32] Anterior oblique fields as compared to lateral opposed fields for passive scattering PT to the prostate and proximal seminal vesicles, were, however, found less robust to interfraction motion.[27]

With the plan selection approach developed in the current study, we obtained statistically significant lower gEUD to the rectum, bladder, and the bowels, and we expect that this could also translate into a clinical gain. However, the clinical impact of the sparing would have to be investigated through a clinical trial. Online adaptive replanning, instead of plan selection, has a potential to further reduce the dose to surrounding tissue. This, however, is more resource intensive than plan selection and with still unresolved technological challenges, for example, on imaging quality for dose calculation and contouring.[11] Plan selection in the current study was facilitated from the use of predefined contours of the targets in the rCTs. This could have affected both the distribution of plans selected and the consistency in the plan selection between different selectors, which was high (>90%). As an alternative, the residual motion vector as defined in the method could be used directly for selecting the plan of the day. The selected plans on a scatter plot of the residual motion for all testing patients is displayed in Figure E3 (available online at https://doi.org/10.1016/j.ijrobp.2019.11.007). This vector can be derived from CBCT or even from orthogonal kV-kV registered on both GM- and BA-registrations. Using images with poorer soft-tissue contrast do, however, limit evaluation of geometric coverage caused by a deforming target. The additional resources in online replanning should also be weighed against the clinical gain from the additional interventions. With the recent advances in automatic planning, the resources needed for creating a plan library can be considerably reduced.

Conclusions

Plan selection from plan libraries derived from a population model of day-to-day motion was feasible for all testing patients. Compared with the nonadaptive delivery approach, plan selection reduced dose to the rectum and bladder without compromising coverage for the targets involved in the selection.

References

1. Trofimov A, Nguyen PL, Efstathiou JA, et al. Interfractional variations in the setup of pelvic bony anatomy and soft tissue, and their implications on the delivery of proton therapy for localized prostate cancer. *Int J Radiat Oncol Biol Phys* 2011;80:928-937.
2. Widesott L, Pierelli A, Fiorino C, et al. Helical tomotherapy vs. intensity-modulated proton therapy for whole pelvis irradiation in high-risk prostate cancer patients: Dosimetric, normal tissue complication probability, and generalized equivalent uniform dose analysis. *Int J Radiat Oncol Biol Phys* 2011;80:1589-1600.
3. Thörnqvist S, Muren LP, Bentzen L, et al. Degradation of target coverage due to inter-fraction motion during intensity-modulated proton therapy of prostate and elective targets. *Acta Oncol* 2013;52:521-527.
4. Hild S, Graeff C, Rucinski A, et al. Scanned ion beam therapy for prostate carcinoma: Comparison of single plan treatment and daily plan-adapted treatment. *Strahlenther Onkol* 2016;192:118-126.
5. Shih HA, Harisinghani M, Zietman AL, et al. Mapping of nodal disease in locally advanced prostate cancer: rethinking the clinical target volume for pelvic nodal irradiation based on vascular rather than bony anatomy. *Int J Radiat Oncol Biol Phys* 2005;63:1262-1269.
6. Lawton CA, Michalski J, El-Naqa I, et al. RTOG GU radiation oncology specialists reach consensus on pelvic lymph node volumes for high-risk prostate cancer. *Int J Radiat Oncol Biol Phys* 2009;74:383-387.
7. Smithmans MH, de Bois J, Sonke JJ, et al. Residual seminal vesicle displacement in marker-based image-guided radiotherapy for prostate cancer and the impact on margin design. *Int J Radiat Oncol Biol Phys* 2011;80:590-596.
8. van der Wielen GJ, Mutanga TF, Incrocci L, et al. Deformation of prostate and seminal vesicles relative to intraprostatic fiducial markers. *Int J Radiat Oncol Biol Phys* 2008;72:1604-1611.
9. Jagt T, Breedveld S, van Haveren R, et al. An automated planning strategy for near real-time adaptive proton therapy in prostate cancer. *Phys Med Biol* 2018;63:135017.
10. Zhang M, Westerly DC, Mackie TR. Introducing an on-line adaptive procedure for prostate image guided intensity modulate proton therapy. *Phys Med Biol* 2011;56:4947-4965.
11. Thörnqvist S, Hysing LB, Tuomikoski L, et al. Adaptive radiotherapy strategies for pelvic tumors — a systematic review of clinical implementations. *Acta Oncol* 2016;55:943-958.
12. Xia P, Qi P, Hwang A, et al. Comparison of three strategies in management of independent movement of the prostate and pelvic lymph nodes. *Med Phys* 2010;37:5006-5013.
13. Heijkoop ST, Langerak TR, Quint S, et al. Clinical implementation of an online adaptive plan-of-the-day protocol for nonrigid motion management in locally advanced cervical cancer IMRT. *Int J Radiat Oncol Biol Phys* 2014;90:673-679.
14. Tuomikoski L, Collan J, Keyriläinen J, et al. Adaptive radiotherapy in muscle invasive urinary bladder cancer—an effective method to reduce the irradiated bowel volume. *Radiother Oncol* 2011;99:61-66.
15. Vestergaard A, Muren LP, Lindberg H, et al. Normal tissue sparing in a phase II trial on daily adaptive plan selection in radiotherapy for urinary bladder cancer. *Acta Oncol* 2014;53:997-1004.
16. Foroudi F, Wong J, Kron T, et al. Online adaptive radiotherapy for muscle-invasive bladder cancer: Results of a pilot study. *Int J Radiat Oncol Biol Phys* 2011;81:765-771.
17. Meijer GJ, de Klerk J, Bzdusek K, et al. What CTV-to-PTV margins should be applied for prostate irradiation? Four-dimensional quantitative assessment using model-based deformable image registration techniques. *Int J Radiat Oncol Biol Phys* 2008;72:1416-1425.
18. Gay HA, Barthold HJ, O'Meara E, et al. Pelvic normal tissue contouring guidelines for radiation therapy: A Radiation Therapy Oncology Group consensus panel atlas. *Int J Radiat Oncol Biol Phys* 2012;83:e353-e362.
19. Hysing LB, Ekanger C, Zolnay A, et al. Statistical motion modelling for robust evaluation of clinically delivered accumulated dose distributions after curative radiotherapy of locally advanced prostate cancer. *Radiother Oncol* 2018;128:327-335.
20. Hysing LB, Söhn M, Muren LP, et al. A coverage probability based method to estimate patient-specific small bowel planning volumes for use in radiotherapy. *Radiother Oncol* 2011;100:407-411.
21. Stroom JC, de Boer HC, Huizenga H, et al. Inclusion of geometrical uncertainties in radiotherapy treatment planning by means of coverage probability. *Int J Radiat Oncol Biol Phys* 1999;43:905-919.
22. van Herk M, Remeijer P, Rasch C, et al. The probability of correct target doseage: Dose-population histograms for deriving treatment margins in radiotherapy. *Int J Radiat Oncol Biol Phys* 2000;47:1121-1135.
23. Thörnqvist S, Hysing LB, Zolnay AG, et al. Treatment simulations with a statistical deformable motion model to evaluate margins for multiple targets in radiotherapy for high-risk prostate cancer. *Radiother Oncol* 2013;109:344-349.
24. Poulsen PR, Muren LP, Høyer M. Residual set-up errors and margins in on-line image-guided prostate localization in radiotherapy. *Radiother Oncol* 2007;85:201-206.
25. Shah AP, Kupelian PA, Willoughby TR, et al. An evaluation of intrafraction motion of the prostate in the prone and supine positions using electromagnetic tracking. *Radiother Oncol* 2011;99:37-43.
26. Lawton CA, Michalski J, El-Naqa I, et al. Variation in the definition of clinical target volumes for pelvic nodal conformal radiation therapy for prostate cancer. *Int J Radiat Oncol Biol Phys* 2009;74:377-382.
27. Moteabbed M, Trofimov A, Sharp GC, et al. Proton therapy of prostate cancer by anterior-oblique beams: Implications of setup and anatomy variations. *Phys Med Biol* 2017;62:1644-1660.
28. Maeda Y, Sato Y, Minami H, et al. Positioning accuracy and daily dose assessment for prostate cancer treatment using in-room CT image guidance at a proton therapy facility. *Med Phys* 2018;45:1832-1843.
29. Paganetti H. Range uncertainties in proton therapy and the role of Monte Carlo simulations. *Phys Med Biol* 2012;57:R99-R117.
30. Meyer J, Bluett J, Amos R, et al. Spot scanning proton beam therapy for prostate cancer: treatment planning technique and analysis of consequences of rotational and translational alignment errors. *Int J Radiat Oncol Biol Phys* 2010;78:428-434.
31. Park PC, Zhu XR, Lee AK, et al. A beam-specific planning target volume (PTV) design for proton therapy to account for setup and range uncertainties. *Int J Radiat Oncol Biol Phys* 2012;82:e329-e336.
32. Andersen AG, Casares-Magaz O, Petersen J, et al. Beam angle evaluation to improve inter-fraction motion robustness in pelvic lymph node irradiation with proton therapy. *Acta Oncol* 2017;56:846-852.